Title

Thermodynamic analysis of a compressed carbon dioxide energy storage system using two saline aquifers at different depths as storage reservoirs

Authors
Liu, Hui
He, Qing
Borgia, Andrea
et al.

Publication Date
2016-11-01

DOI
10.1016/j.enconman.2016.08.096

Peer reviewed

Thermodynamic analysis of a compressed carbon dioxide energy storage system using two saline aquifers at different depths as storage reservoirs

Hui Liu[1,2], Qing He[1], Andrea Borgia[2], Lehua Pan [2], Curtis M. Oldenburg[2*]

[1]School of Energy Power and Mechanical Engineering,
North China Electric Power University,
[2]Beinong Road, Changping, Beijing 102206
China
[2]Energy Geosciences Division, 74-316C
Lawrence Berkeley National Laboratory
Berkeley, CA 94720
USA

Corresponding author: Curtis M. Oldenburg,
Energy Geosciences Division, 74-316C
Lawrence Berkeley National Laboratory
Berkeley, CA 94720
USA
Email address: cmoldenburg@lbl.gov

Citation for this paper:

Liu, H., He, Q., Borgia, A., Pan, L. and Oldenburg, C.M., 2016. Thermodynamic analysis of a compressed carbon dioxide energy storage system using two saline aquifers at different depths as storage reservoirs. Energy Conversion and Management, 127, pp.149-159.

Abstract: Compressed air energy storage (CAES) is one of the leading large-scale energy storage technologies. However, low thermal efficiency and low energy storage density restrict its application. To improve the energy storage density, we propose a two-reservoir compressed CO_2 energy storage system. We present here thermodynamic and parametric analyses of the performance of an idealized two-reservoir CO_2 energy storage system under supercritical and transcritical conditions using a steady-state mathematical model. Results show that the transcritical compressed CO_2 energy storage system has higher round-trip efficiency and exergy efficiency, and larger energy storage density than the supercritical compressed CO_2 energy storage. However, the configuration of supercritical compressed CO_2 energy storage is simpler, and the energy storage densities of the two systems are both higher than that of CAES, which is advantageous in terms of storage volume for a given power rating.

Key words: Subsurface energy storage; Compressed CO_2 energy storage system; Utilization of CO_2; Two saline aquifers reservoirs； Thermodynamic analysis; Parametric analysis.

Nomenclature

H	enthalpy, kJ/kg
S	entropy, kJ/(kg·K)
P	pressure, MPa
$\dot{E}$	exergy, kW
T	temperature, K
T_s	surface temperature, K
W	shaft work, kW
C_{p}	specific heat capacity at constant pressure, kJ/(kg·K)
G	geothermal gradient, K/km
V	volume, m^3
$\dot{m}$	mass flow rate, kg/s
$\dot{Q}$	heat transfer, W
Z	depth of saline reservoir, m
Abbreviations	
A-CAES	adiabatic CAES
AA-CAES	advanced adiabatic CAES
C	compressor
CAES	compressed air energy storage
CCES	compressed CO_2 energy storage
HE	heater
HS	high pressure reservoir

LS	low pressure reservoir
PM-CAES	porous media CAES
RE	recuperator
SC-CCES	supercritical compressed CO_2 energy storage
SC-CO_2	supercritical CO_2
T	turbine
TC-CCES	transcritical compressed CO_2 energy storage
TC-CO_2	transcritical CO_2
Greek symbols	
β_p	pore compressibility, Pa^{-1}
β_w	change in brine density
η	efficiency
τ	temperature difference，K
ρ	density, kg/m^3
Subscripts	
S	isentropic process
Comp	compressor
1	inlet stream
2	outlet stream
T	turbine
NG	nature gas
F	fuel

tot	total
D	destruction
L	loss

1. Introduction

In recent years, renewable energy, particularly wind power and solar photovoltaic (PV) generation has demonstrated robust growth-worldwide motivated by concerns about energy security and climate change due to CO_2 emission levels[1-2]. But Renewable energy sources (e.g., solar and wind energy) exhibit significant and uncontrollable intermittency during power production. When these renewable energy sources are connected to an electrical grid, they can cause serious safety problems for the grid; hence, it is difficult to deliver power from renewable energy sources that instantly matches electricity demand[3].

To solve this dilemma and develop renewable energy sources further, viable energy storage systems (ESS) are required. For example, an efficient ESS can increase the penetration of wind power generation by controlling wind power plant output and storage, in addition to providing ancillary services to the power system[4-5].

On a utility scale, compressed air energy storage (CAES) is one of the technologies with the highest economic feasibility with potential to contribute to a flexible energy system with an improved utilization of intermittent renewable energy sources[1]. The feasibility of using CAES to integrate fluctuating renewable power into the electricity grid has been proven by many researchers[6-9]. Bosio and Verda[6] analyzed the thermo-economics of a CAES system integrated into a wind power plant in the framework of the Italian Power Exchange market, which showed that a hydroelectric power plant (HPP)-CAES system was cost-effective in terms of solving local imbalances of the grid. Clearly et al.[7] evaluated the economic benefits of CAES in mitigating wind curtailment. They showed that both wind curtailment levels and wind-farm total annual generation costs could be decreased. Arabkoohsar et al.[8-9] simulated and analyzed CAES equipped with a solar heating system. The results showed that CAES could increase the efficiency and reliability of a PV plant.

However, the main drawbacks of a CAES system include its low thermal efficiency (e.g., Huntorf CAES plant efficiency is 42% and AA-CAES efficiency is about 70%[10]), CO_2 emissions from combustion of natural gas in the recovery system for conventional CAES, the need for high temperature thermal storage and temperature resistant materials for adiabatic CAES (A-CAES). These factors limit further development of CAES. Although large-scale caverns are also required for CAES as it is carried out today, porous media systems such as aquifers and depleted natural gas reservoirs, so-called porous media CAES (PM-CAES) systems, offer much more storage capacity[11].

Thermodynamic analyses of CAES systems have been performed to optimize these systems and improve their thermal efficiency. For example, Buffa et al.[12] conducted an exergy analysis of A-CAES and found that exergy destruction mostly occurred in the compressors and coolers. Proczka et al.[13] analyzed the effects of pressure and the efficient sizing of pressure vessels on CAES. Zhang et al.[14-15] analyzed the thermodynamic effects of thermal energy storage (TES) and the air storage chamber model on a CAES system. Jubeh and Najjar et al.[16] explored the effects of operating variables on A-CAES performance. Najjar and Zamout analyzed the effects of dry regions on the performance of a CAES plant[17]. The operation, experience, and characteristics of Huntorf CAES were also investigated[18]. Thermodynamic analyses have shown that, both, decreasing the exhaust temperature and using heat of compression during expansion can significantly improve CAES efficiency.

Several novel CAES systems have been proposed that reduce waste heat. A recuperator was utilized to capture heat from the turbine exhaust, which could reduce the fuel consumption of the McIntosh plant by 25%[19-20]. Safaei and Keith[17] proposed a distributed CAES (D-CAES) system that placed compressors near heat demand loads to recover the heat generated during the compression stage. Liu[2] proposed a modified A-CAES system that used a pneumatic motor instead of a low pressure turbine (LT) to reduce the exhaust temperature caused by LT, and the exergy efficiency can be improved by nearly 3% compared with that of the conventional A-CAES system. Guo et al.[21] proposed a novel A-CAES system in which an ejector was integrated into an A- CAES system to recover pressure reduction losses; energy conversion efficiency could reach 65.36%. Several demonstration A-CAES plants have been built, such as a 1.5 MW A-CAES in China, where initial experimental tests are on-going. An A-CAES technology that uses reversible reciprocating piston machines is being developed by LightSail Energy Ltd. in the U.S. Other new systems include a tri-generation system based on compressed air and thermal energy storage[22], biomass-fueled CAES, isobaric adiabatic CAES with combined cycle[23], combined cooling, heating and power system based on small-scale CAES[24], CAES using a cascade of phase change materials[25], CAES combined with solar thermal capture[26], integrating CAES with diesel engine[27], and compressed carbon dioxide energy storage[28].

Although thermal efficiency can be improved by various methods, CAES has low energy density and requires large-scale storage reservoirs[29]. To overcome these restrictions, several studies have been conducted on novel energy storage technologies. For instance, Kim[30] proposed a constant-pressure CAES system combined with pumped hydro-storage to reduce the cavern volume. Guo et al.[31] presented a supercritical compressed air energy storage (SC-CAES). Oldenburg and Pan[11] modeled a porous media CAES (PM-CAES) system that uses aquifers or depleted natural gas reservoirs for storage. Underwater compressed air energy storage (UWCAES) stores the compressed air under water by using a large elastic bladder[32]. Small scale CAES (SS-CAES) that stores high-pressure air in a tank or an underground pipeline was also proposed[33]. Each of these novel approaches brings with it additional requirements and limitations.

As popularly known, CAES is derived from the Brayton cycles, and gases like CO_2

that are non-ideal at operating conditions are more efficient in a Brayton cycle[34].

Using CO_2 as the working fluid in a compressed gas energy storage system can also achieve better performance than AA-CAES[35]. At the same time geological CO_2 sequestration in deep formations (e.g., saline aquifers, gas and oil reservoirs, and coal beds) is a promising measure for reducing greenhouse gas emissions[36]. Therefore, the combination of compressed gas energy storage in the deep subsurface and large-scale utilization of CO_2 is both possible and beneficial.

Although, some research has been conducted on energy power cycle and energy storage systems based on CO_2 and liquid CO_2[28,35], we are not aware of published analyses of energy storage systems based on transcritical CO_2 (transition from supercritical to gas) or based on supercritical CO_2 throughout the cycle. Therefore, the innovation of this paper resides in the exergy analysis of a closed-loop gas storage system, conceived by two of us (Borgia and Oldenburg in January of 2012), which comprises two reservoirs, in this case in saline aquifers but which could also be in caverns, located at different depths and uses transcritical and supercritical CO_2 as the working fluid. This novel energy storage system can be used in two different energy cycles (e.g., transcritical CO_2 energy storage cycle, and supercritical CO_2 energy storage cycle) according to the physical state of CO_2 in the process. We conducted energy and exergy analyses to understand the thermal properties of the compressed CO_2 energy storage system. In addition, parametric analysis was performed to investigate the effects of the physical conditions of two saline aquifer reservoir (e.g., energy storage pressure, energy releasing pressure, and pressure of low-pressure reservoir) on system performance.

2. System description

The proposed compressed CO_2 energy storage system using two saline aquifers as storage reservoirs is a closed energy-storage cycle. The first reservoir is a low-pressure reservoir used to store CO_2 exhausted from the turbine, whereas the second reservoir is at higher pressure to store CO_2 from the compressor. This energy storage system, although based on the same principles, can be operated in two different ways according to the state of CO_2, (1) by allowing the CO_2 to transition from supercritical to gaseous conditions in the turbine, which we refer to as the transcritical compressed CO_2 energy storage (TC-CCES) system, and (2) by keeping the CO_2 above the critical pressure throughout the cycle, which we refer to as the supercritical compressed CO_2 energy storage (SC-CCES) system. The schematic and *T-S* diagram of compressed CO_2 energy storage (CCES) is shown in Figs. 1 and 2.

1: During off-peak hours, the working fluid (low-pressure CO_2) stored in a shallow low-pressure reservoir is removed, pressurized, and injected into a deeper high-pressure reservoir using surplus renewable power, such as that from wind or solar.

2: For multi-stage compressor, the heat of compression of the CO_2 is absorbed by a cooling fluid which is stored in a TES system, while the CO_2 from the last stage compressor is directly injected into the high-pressure storage reservoir.

3: During peak hours, the high-pressure CO_2 is regulated to a certain pressure through the throttle valve, and is transported to the recuperator system to absorb the heat exhausted from the turbine in the TES.

4: The heated high-pressure CO_2 is fed into the turbine.

5: The high pressure CO_2 expands through the turbine generating shaft work.

6: The exhaust CO_2 is stored in the low-pressure reservoir.

Considering that because of the geothermal gradient the temperature of the saline-aquifer reservoirs increases with depth, the output CO_2 from the compressor stage can be directly injected into the high-pressure reservoir storing, both heat and CO_2 directly into the rock formation. Therefore, the proposed SC-CCES does not need a TES to store the compressed heat generated during compression, implying that the aftercooler is theoretically unnecessary. In our analysis, though, to allow a direct comparison with CAES and highlight the benefits of the two-reservoir CCES system, we retain the heater.

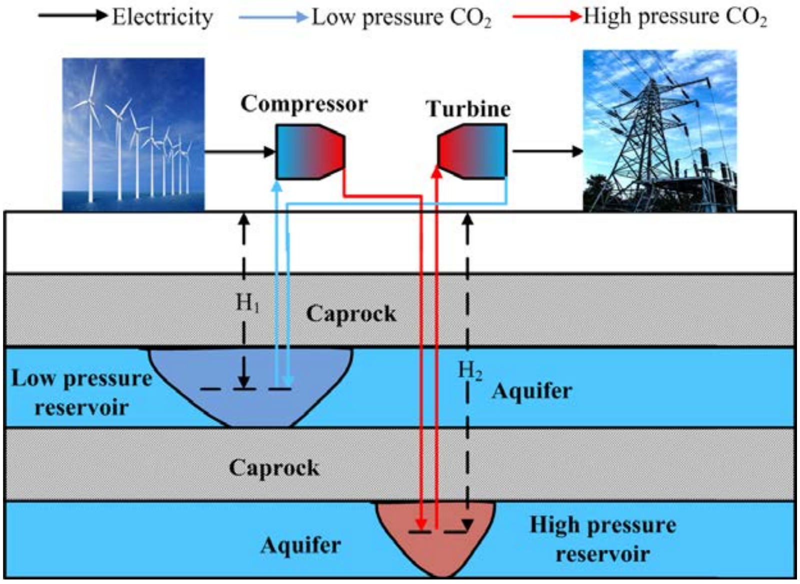

Fig.1. Schematic illustration of CCES using two saline-aquifer reservoirs.

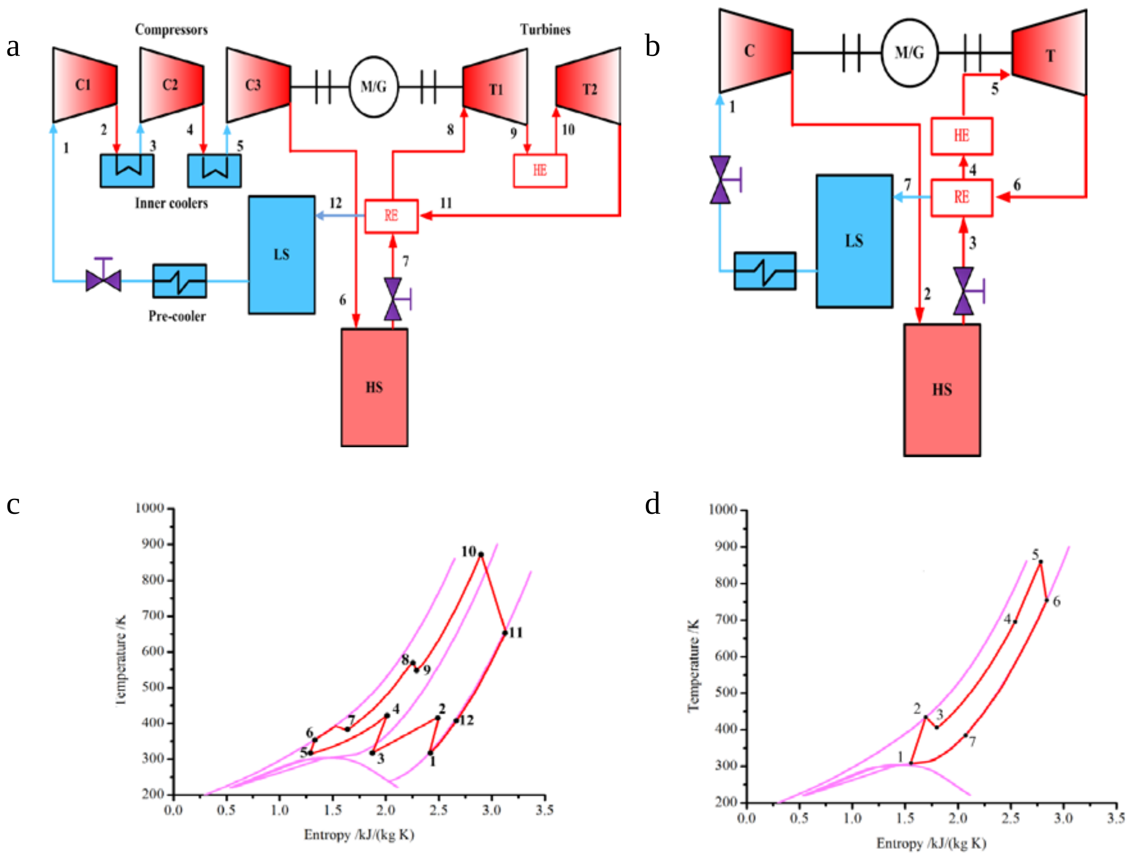

Fig.2. CCES using two saline aquifers reservoirs. a. The schematic of TC-CCES. b. The schematic of SC-CCES. c. *T-S* diagram of TC-CCES. d. *T-S* diagram of SC-CCES. C = compressor; RE = recuperator; T = turbine; HE = heater; LS = low pressure reservoir; and HS = high pressure reservoir.

3. Theoretical model

The following assumptions are made to simplify the theoretical model of the compressed CO_2 energy storage cycle:

1. The pressure drop and heat loss in the pipes, heat exchanger, TES, and recuperator are ignored.
2. The compressor and the turbine have a given isentropic efficiency.
3. Changes in kinetic energy and potential energy are negligible relative to the stored energy.
4. The storage in the two saline aquifers is considered a closed system at hydrostatic pressure.
5. The mass flow rate of CO_2 is the same in the storage and recovery modes of operation, and for TC-CCES and SC-CCES.

3.1. Compressor model

The isentropic efficiency of compressor η_{comp} is,

$$\eta_{\mathrm{comp}} = \frac{h_{2\mathrm{s}} - h_1}{h_2 - h_1}, \tag{1}$$

where h_1 is inlet enthalpy and $h_{2\mathrm{s}}$ is outlet enthalpy during isentropic compression, h_2 is the real enthalpy during compression.

During isentropic compression, the entropies of the initial and final states are the same, i.e.,

$$s_{2s} = s_1, \tag{2}$$

The corresponding enthalpy of the outlet stream at the end of isentropic compression can be calculated from the property relationship, *f*, which is derived from the equation of state,

$$h_{2s} = f\left(s_{2s}, p_2\right), \tag{3}$$

The actual enthalpy of the pressurized CO_2 at the outlet of the compressor can be calculated using the definition of compression efficiency. Hence, the power consumed, w_{comp}, is,

$$w_{\text{comp}} = h_2 - h_1, \tag{4}$$

3.2. Heat exchanger model

The properties, such as density, specific heat, and viscosity are observed to undergo drastic variations within a very narrow range of temperature if the CO_2 is under supercritical pressure, which will have a great effect on system performance. Therefore, it is essential to divide the heat exchanging process into adequately small sections, such that property variations in each section are so small that constant properties can be assumed [37].

The inner cooler, pre-cooler, and recuperator function together as the heat exchanger. For the inner and pre-cooler, we assumed that the upper terminal temperature difference $\Delta\tau_{\text{upper}}$, and inner and pre-cooler temperatures are both constant. To obtain the amount of compressed heat, the overall temperature change for CO_2 is divided into N equal differences $\Delta\tau$. The specific heat at constant pressure at each intermediate state is determined from the known pressure and temperature. The heat transfer for each step *i* and mass flow rate of water are calculated from the following equations:

$$\dot{Q}_i = \dot{m}_{\mathrm{CO_2}} C_{\mathrm{P,CO_2},i} \left(\tau_{\mathrm{CO_2},i+1} - \tau_{\mathrm{CO_2},i}\right), \tag{5}$$

$$\dot{Q}_i = \dot{m}_{\mathrm{water}} C_{\mathrm{P,water},i} \left(\tau_{\mathrm{water},i+1} - \tau_{\mathrm{water},i}\right), \tag{6}$$

$$\dot{m}_{\mathrm{water}} = \frac{\sum_{i}^{N} \dot{Q}_i}{(h_{\mathrm{water,out}} - h_{\mathrm{water,in}})} \quad , \tag{7}$$

For the recuperator, we assumed that lower terminal temperature difference, $\Delta\tau_{\mathrm{lower}}$, is constant. Also the enthalpy change for hot streams is divided into *N* equal differences Δh. The cooling working fluid temperatures of preheater and recuperator at each intermediate state can be determined using the CoolProp database from the known enthalpy and pressure.

3.3. Aquifer CO_2 storage model

To inject CO_2 into a saline aquifer reservoir, the CO_2 pressure has to be at least as high as the initial groundwater pressure in the reservoir. In the present study, the CO_2 pressures in the low-pressure reservoir and high-pressure reservoir are assumed to exhibit hydrostatic variation with depth at a constant pressure gradient.

The geothermal gradient (underground temperature increases with depth) will control the temperature of the reservoir. Using values for the surface temperature and geothermal gradient, the underground temperature as a function of depth can be determined by,

$$T = T_s + Gz \,, \tag{8}$$

where T_s is the surface temperature; G is the geothermal gradient; z is the depth.

We assume the saline aquifer is a closed-storage formations[36]. To estimate aquifer storage reservoir volume, V_S, the following equation is used,

$$V_S = \frac{M_{CO_2}}{(\beta_P + \beta_W)\rho_{CO_2}\Delta P} \,, \tag{9}$$

where M_{CO2} and ρ_{CO_2} are respectively the mass and density of CO_2 at reservoir conditions; Δp is the pressure buildup from beginning to the end of injection; β_p is the pore compressibility; β_w is the change in brine density.

3.4. Turbine model

The calculation method for the actual expansion is the same as that for compression. The isentropic efficiency of the turbine can be calculated using,

$$\eta_t = \frac{h_3 - h_{4s}}{h_3 - h_4} \,, \tag{10}$$

The entropies of the initial and final states are the same during isentropic expansion, i.e.,

$$s_{4s} = s_3 \,, \tag{11}$$

The corresponding enthalpy of the outlet stream at the end of isentropic expansion can be calculated from the property relationship, f, which is derived from the equation of state. That is,

$$h_{4s} = f\left(s_{4s}, p_4\right) , \tag{12}$$

The actual enthalpy of the pressurized CO_2 at the outlet of the compressor can be calculated using the definition of expansion efficiency. Thus, expansion work can be calculated using,

$$w_{\mathrm{T}} = h_3 - h_4\,, \tag{13}$$

4. Performance`criteria

To analyze the performance of compressed CO_2 energy storage using two saline aquifers as reservoirs, exergy efficiency, exergy destruction, round-trip efficiency, and energy storage density are introduced as the performance criteria of the overall system and the main components[2,38].

4.1. Energy analysis

4.1.1. Round-trip efficiency

To facilitate comparisons of the novel energy storage system to other electrical storage devices, the round-trip efficiency of energy storage is defined as[38-39],

$$\eta_{RT,1} = \frac{E_{\mathrm{T}}}{E_{\mathrm{C}} + \eta_{\mathrm{NG}} E_{\mathrm{F}}}\,, \tag{14}$$

where E_{T} represents the electricity output; E_{C} represents the electricity input; $\eta_{\mathrm{NG}}E_{\mathrm{F}}$ represents the amount of electricity that could have been made from the natural gas input E_{F}, if that fuel had been used to make electricity in a stand-alone power plant at efficiency η_{NG} instead of to fire an energy storage unit, $\eta_{\mathrm{NG}} = 47.6\%$[38].

4.1.2. Energy storage density

Determining the amount of electrical energy that can be produced per unit volume of storage capacity (E_{GEN}/V_S) is essential to evaluate the geological requirements for compressed gas energy storage. The energy produced per unit volume for compressed CO_2 energy storage with two saline reservoirs is,

$$E_{\mathrm{GEN}}/V_{\mathrm{S}} = \frac{w_{\mathrm{t}}\left(\beta_{\mathrm{P}} + \beta_{\mathrm{W}}\right)\left(\rho_{1,\mathrm{CO_2}}\Delta P_1 + \rho_{2,\mathrm{CO_2}}\Delta P_2\right)}{2}, \tag{15}$$

4.2. Exergy analysis

The general exergy balance for the overall system is[40-41],

$$\dot{E}_{\mathrm{F,tot}} = \dot{E}_{\mathrm{P}} + \sum_k \dot{E}_{\mathrm{D},k} + \dot{E}_{\mathrm{L}}, \tag{16}$$

where $\dot{E}_{\mathrm{F,tot}}$, $\dot{E}_{\mathrm{P}}$, $\sum_k \dot{E}_{\mathrm{D},k}$, and $\dot{E}_{\mathrm{L}}$ represent the total amount rate of fuel exergy, product exergy, exergy destruction, and exergy loss associated with the overall considered system, respectively.

The general exergy balance of the k^{th} component of the overall system can be expressed as follow:

$$\dot{E}_{\mathrm{D},k} = \dot{E}_{\mathrm{F},k} - \dot{E}_{\mathrm{P},k}, \tag{17}$$

where $\dot{E}_{D,k}$, $\dot{E}_{F,k}$, and $\dot{E}_{P,k}$ represent the exergy destruction rate, the fuel exergy, and the product exergy rate within the k^{th} component, respectively. Exergy efficiency is defined as,

$$\eta_{\mathrm{ex}} = \frac{E_{\mathrm{F,tot}} - \sum E_{\mathrm{D},k} - E_{\mathrm{L}}}{E_{\mathrm{F,tot}}} = \frac{E_{\mathrm{p}}}{E_{\mathrm{F,tot}}}, \tag{18}$$

Exergy destruction in each component of the system can be calculated using the equations listed in Table 1. To compare the exergy destruction of dissimilar components, the exergy destruction ratio of the k^{th} component is defined as

$$y^{*}_{\mathrm{D},k} = \frac{\dot{E}_{\mathrm{D},k}}{\dot{E}_{\mathrm{D},tot}}, \tag{19}$$

Table 1. Exergy calculation in each component of the novel system.

Component	Schematic view	$\dot{E}_{\mathrm{F},k}$	$\dot{E}_{\mathrm{P},k}$	$\dot{E}_{\mathrm{D},k}$
Compressors	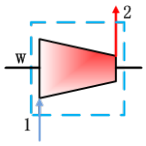	W	$\dot{E}_{2,\mathrm{C}} - \dot{E}_{1,\mathrm{C}}$	$\dot{E}_{\mathrm{F,C}} - \dot{E}_{\mathrm{P,C}}$
Storage cavern	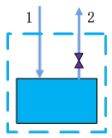	$\dot{E}_{1,\mathrm{SC}}$	$\dot{E}_{2,\mathrm{SC}}$	$\dot{E}_{\mathrm{F,SC}} - \dot{E}_{\mathrm{P,SC}}$
Heater	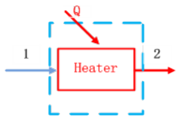	$\dot{E}_{\mathrm{Q,H}}$	$\dot{E}_{2,\mathrm{H}} - \dot{E}_{1,\mathrm{H}}$	$\dot{E}_{\mathrm{F,H}} - \dot{E}_{\mathrm{P,H}}$
Heat exchanger	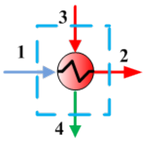	$\dot{E}_{3,\mathrm{HE}} - \dot{E}_{4,\mathrm{HE}}$	$\dot{E}_{2,\mathrm{HE}} - \dot{E}_{1,\mathrm{HE}}$	$\dot{E}_{\mathrm{F,HE}} - \dot{E}_{\mathrm{P,HE}}$
Turbine	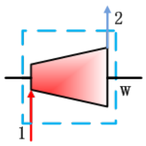	$\dot{E}_{1,\mathrm{T}} - \dot{E}_{2,\mathrm{T}}$	W	$\dot{E}_{\mathrm{F,T}} - \dot{E}_{\mathrm{P,T}}$

5. Results and discussions

The simulations for the parametric analysis of the compressed transcritical and supercritical CO_2 energy storage are carried out using a MATLAB™ with the thermodynamic properties of the working fluid calculated through CoolProp[42]. The design parameters and detailed conditions for the simulation and analysis of the compressed gas energy storage are summarized in Table 2.

5.1. Thermodynamic analysis

The detailed results of the analysis of compressed CO_2 energy storage using two saline aquifers as reservoirs are presented in Tables 3 and 4, which show the thermodynamic parameters at each node of the two storage systems, respectively. A summary of the results of the energy and exergy analyses are provided in Table 5. The round-trip efficiency and exergy efficiency of compressed transcritical CO_2 energy storage is better than those of the compressed supercritical CO_2 energy storage. Moreover, the compressed transcritical CO_2 energy storage has a higher energy density (E_{GEN}/V_S) than the compressed supercritical CO_2 energy storage. In addition, the energy densities (E_{GEN}/V_S) of the two systems can reach 497.68 kWh/m^3 (transcritical CO_2) and 255.20 kWh/m^3 (supercritical CO_2), which are better compared with that for CAES (E_{GEN}/V_S = 2-20 kWh/m^3)[38] because more energy can be stored in a given reservoir. The reason that the energy storage density using transcritical CO_2 is much larger than that of supercritical CO_2 comes from the fact that the output work of compressed transcritical CO_2 energy storage is more than two times larger than that of compressed supercritical CO_2 energy storage. According to Eq. (15), the energy storage density is mainly a function of w_t under the same reservoir conditions. The w_t of transcritical compressed CO_2 energy storage and supercritical compressed CO_2 energy storage are 254.82 kW and 123.58 kW, respectively. Therefore, the energy storage density using transcritical CO_2 is about two times as large as that of supercritical CO_2 under a pressure of 40 MPa.

Fig. 3 shows the exergy destruction ratio of the different components of the compressed CO_2 energy storage under simulation conditions. For the compressed transcritical CO_2 energy storage, 54.37% of the irreversibility takes place in the heater, 11.98% in the low pressure reservoir, 10.93% in the compressor, 9.78% in the turbine, 9.52% in the recuperator, 3.42% in the high pressure reservoir. However, for the compressed supercritical CO_2 energy storage, the largest exergy destruction is contributed by high pressure reservoir, which exceeds 33.37% of the total exergy destruction of the system. Secondly the heater brings larger exergy destruction, which accounts for 20.98% of total exergy destruction.

Table 2. Parameters setting in the compressed CO_2 energy storage with two reservoirs.

Parameter	Value	Unit
Ambient temperature	308.00	K
Pressure drop in throttle valve in compression process	0.50	MPa
Inlet temperature	313.00	K
Outlet pressure of compressor train	25.00	MPa
Temperature of cooling water	308.00	K
Pressure drop in throttle valve in expansion process	5.00	MPa
Outlet temperature of heater	873.00	K
Outlet pressure of turbine train in supercritical cycle	8.00	MPa
Outlet pressure of turbine train in transcritical cycle	2.00	MPa
Isentropic efficiency of compressor	0.85	/
Isentropic efficiency of turbine	0.87	/
SCO_2 Depth of low pressure reservoir	760.00	M
SCO_2 Depth of high pressure reservoir	3000.00	M
TCO_2 Depth of low pressure reservoir	200.00	M
TCO_2 Depth of high pressure reservoir	3000.00	M

Table 3. Thermodynamic data for the material streams of the compressed transcritical CO_2 energy storage.

Streams	Material stream	T(K)	p(MPa)	h(kJ/kg)	s(kJ/kg·K)	e(kJ/kg)
1	CO_2	308.05	1.50	501.50	2.23	153.86
2	CO_2	405.37	4.49	580.00	2.26	223.17
3	CO_2	313.00	4.49	473.80	1.96	209.00
4	CO_2	413.74	13.43	541.34	1.98	268.86
5	CO_2	313.00	13.43	289.61	1.27	237.68
6	CO_2	345.89	40.18	328.34	1.28	271.07
7	CO_2	382.16	20.00	446.52	1.69	267.18
8	CO_2	587.11	20.00	744.79	2.33	392.83
9	CO_2	540.60	12.62	704.10	2.34	279.87
10	CO_2	873.00	12.62	1101.81	2.91	505.91
11	CO_2	669.75	2.00	873.09	2.96	345.20
12	CO_2	387.16	2.00	574.82	2.39	174.06

Table 4.Thermodynamic data for the material streams of the compressed supercritical CO_2 energy storage.

Streams	Material stream	T(K)	p(MPa)	h(kJ/kg)	s(kJ/kg·K)	e(kJ/kg)
1	CO_2	307.83	7.40	400.71	1.66	228.07
2	CO_2	432.61	40.18	484.96	1.69	302.86
3	CO_2	382.16	20.00	446.52	1.69	267.18
4	CO_2	699.02	20.00	882.22	2.54	437.04
5	CO_2	873.00	20.00	1097.20	2.81	568.41
6	CO_2	763.71	8.04	973.57	2.84	437.31
7	CO_2	387.16	8.04	537.87	2.05	243.42

Table 5. Results of the material streams of the transcritical and supercritical compressed CO_2 energy storage.

Term	Unit	Value of TC-CCES	Value of SC-CCES
C1 power	kW/kg	78.37	83.81
C2 power	kW/kg	67.46	-
C3 power	kW/kg	38.56	-
T1 power	kW/kg	103.62	123.58
T2 power	kW/kg	151.20	-
Thermal energy input	kJ/s	457.70	240.73
Round-trip efficiency	%	63.35	62.28
Exergy efficiency	%	53..02	51.56
E_{GEN}/V_S	kWh/m^3	497.68	255.20

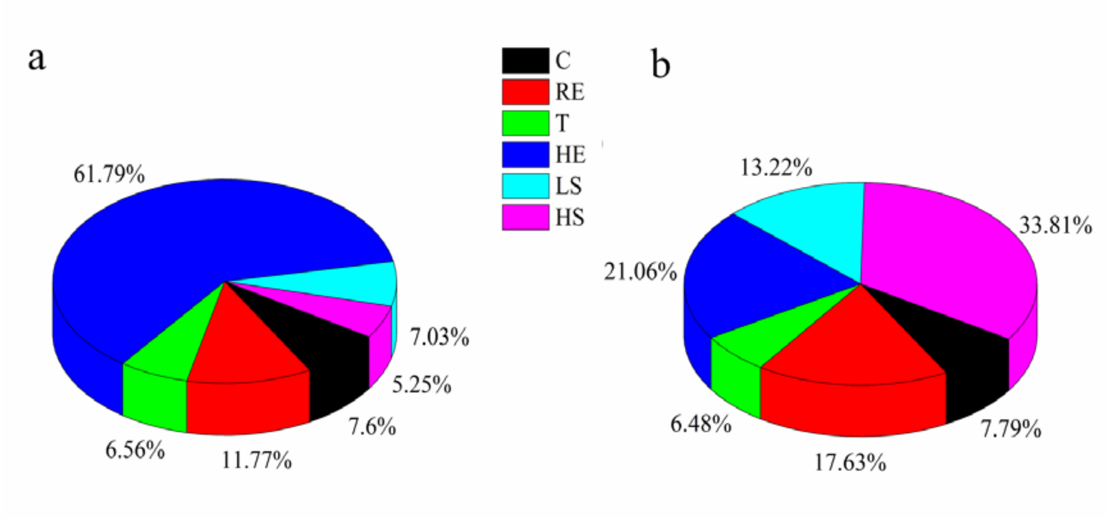

Fig. 3. The exergy destruction ratio of main components. a. transcritical compressed CO_2 energy storage. b. supercritical compressed CO_2 energy storage. C = compressor; RE = recuperator; T = turbine; HE = heater; LS = low pressure reservoir; and HS = high pressure reservoir.

5.2. Sensitivity analysis of key thermodynamic parameters

Based on above analysis, the main advantage of CCES using two saline aquifers reservoirs is the high energy-storage density. Energy storage pressure (outlet pressure of last-stage compressor), release pressure (inlet pressure of first stage-turbine), and pressure of the low-pressure reservoir (outlet pressure of last-stage turbine) are primary and significant parameters that influence the energy storage density. Therefore, conducting a parametric analysis to understand the effects of these various parameters on the performance of the storage system is essential, and parameters range of variation are shown in Table 6.

Table 6. The parameters of the compressed CO_2 energy storage system.

Parameters	Range of variation
Energy storage pressure /MPa	40-56
Energy releasing pressure /MPa	10-26
Pressure of low pressure reservoir /MPa	2-10

5.2.1. Effects of the energy storage pressure

Fig. 4 illustrates the effect of the energy storage pressure on round-trip efficiency and exergy efficiency. The round-trip efficiency and exergy efficiency of the TC-CCES and SC-CCES increase along with the increase in the energy storage pressure. Moreover, the round-trip efficiency and exergy efficiency of SC-CCES are higher than those of TC-CCES when the energy storage pressure is higher than 44 MPa. And the round-trip efficiency is even higher than the exergy efficiency. The reason is that for the round-trip efficiency, the input energy is electricity which includes the consumption electricity of compressors and the conversion terms, as shown in Eq. (14). However, for the exergy efficiency, the input exergy consists of two terms: electricity exergy and thermal exergy, as shown in Eq. (18). According to the second law of thermodynamics, the thermal exergy calculated by the input thermal energy multiplied by the Carnot efficiency. The Carnot efficiency will be larger than the $\eta_{NG,}$ when the other exergy destructions happened in power plant are considered. Therefore, the round-trip efficiency is higher than the exergy efficiency.

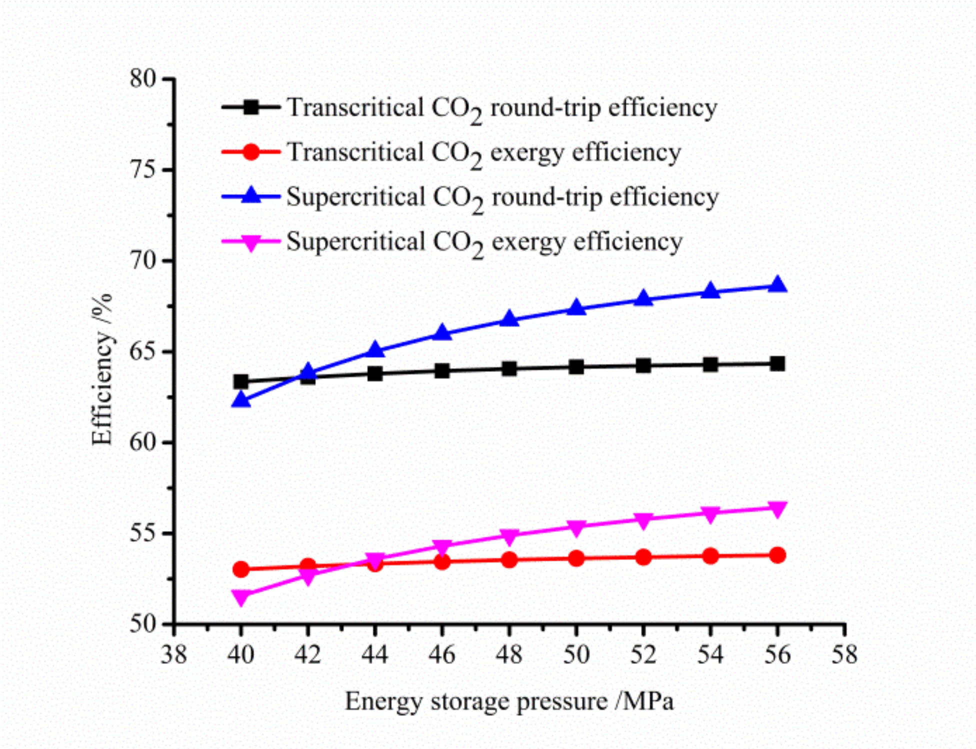

Fig. 4. Effect of energy storage pressure on round-trip efficiency and exergy efficiency.

The effect of energy storage pressure on energy storage density is shown in Fig. 5. An increase in the energy storage pressure increases net energy output during discharge, which can increase energy storage density. According to Eq. (15), energy storage density is determined by the work output during expansion and the volume of the two-saline aquifers reservoirs. A high energy storage pressure will reduce the required volume of the high-pressure reservoir, whereas the change in the work output is opposite to that of required volume. Therefore, energy storage density will increase along with the increase in the energy storage pressure for TC-CCES and SC-CCES.

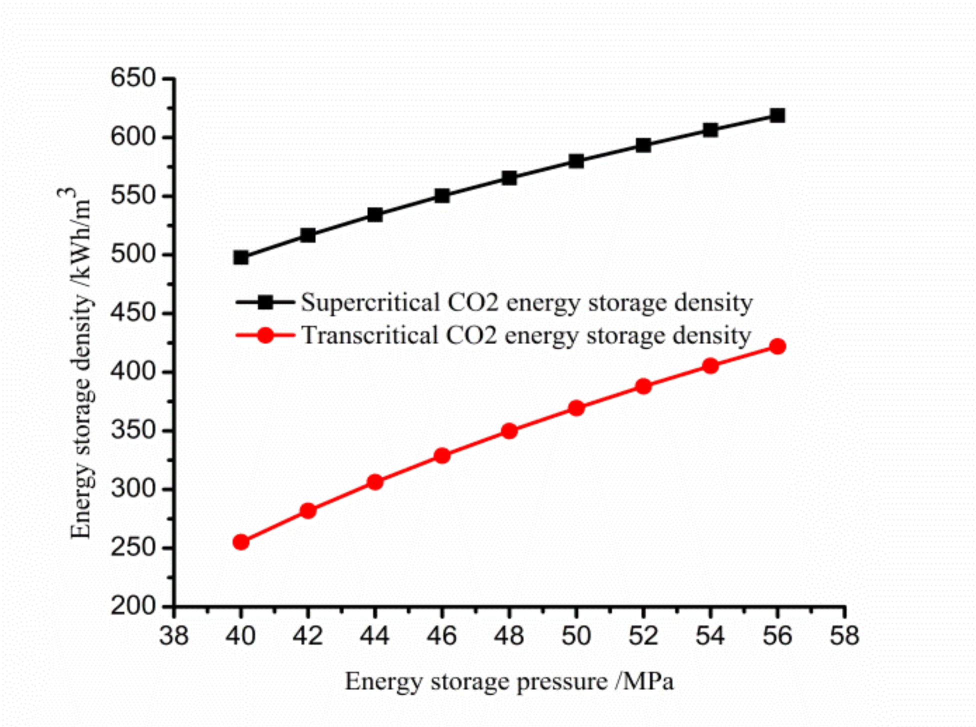

Fig. 5. Effect of the energy storage pressure on the energy storage density.

Fig. 6 shows the effect of the energy storage pressure on the exergy destruction rate of the main components in TC-CCES and SC-CCES, respectively. The results of the exergy analysis indicate that exergy destruction is mainly contributed by HE and RE in TC-CCES, and the largest exergy destruction is contributed by HS, HE and RE in SC-CCES. Moreover, the rate of RE exergy destruction decreases with the increase in the energy storage pressure, whereas the change in the HE exergy destruction rate is opposite to that of RE in the two energy storage systems. The outlet pressure of the turbine is constant; hence, the outlet temperature of the turbine will decrease with the increase in the energy storage pressure, which will result in a smaller temperature difference in RE. A low outlet temperature of the turbine will lead to a low inlet temperature of HE; hence, the temperature difference will be increased. Therefore, more heat is needed to heat the CO_2 in the heater. The exergy destruction of RE is mainly contributed by the temperature difference between hot and cold working fluids. The exergy destruction of HE is not only contributed by the temperature difference, but also by the amount of heat put into the heater. Consequently, the exergy destruction rate of RE will decrease with the increase in the energy storage pressure, whereas that of HE will exhibit the opposite trend. The exergy destruction rate of C, T, LS, HS is caused by the pressure difference, the pressure difference is higher, the exergy destruction is larger. Therefore, the exergy destruction rate will increase with the increase in energy storage pressure when the outlet pressure of turbine is constant.

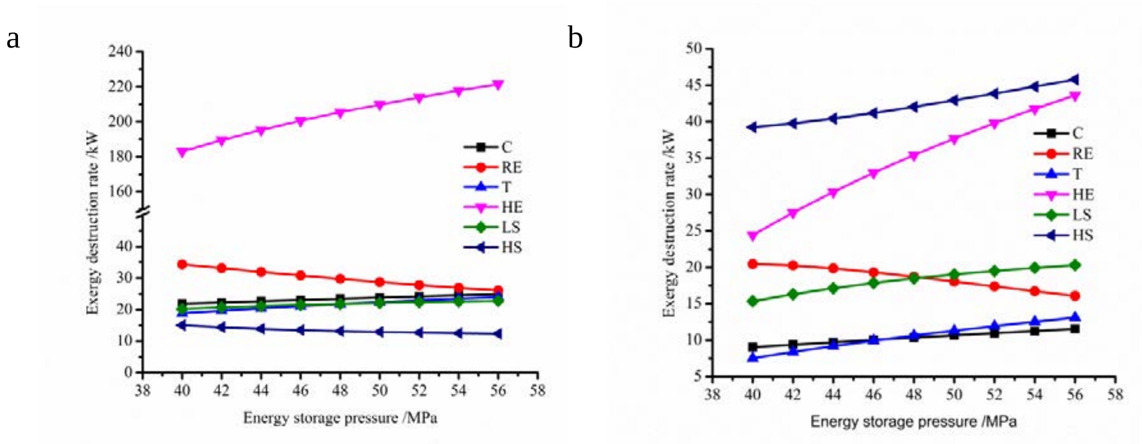

Fig. 6. Effect of energy storage pressure on exergy destruction rate. a. transcritical compressed CO_2 energy storage. b. supercritical compressed CO_2 energy storage. C = compressor; RE = recuperator; T = turbine; HE = heater; LS = low pressure reservoir; and HS = high pressure reservoir.

5.2.2. Effects of energy releasing pressure

The effect of the energy releasing pressure on round-trip efficiency, exergy efficiency, and energy storage density is illustrated in Figs. 7 and 9. The round-trip efficiency and exergy efficiency of TC-CCES and SC-CCES both increase with the increase in energy-release pressure. However, the variation in energy release pressure has a larger effect on the round-trip efficiency and exergy efficiency of SC-CCES. Moreover, the performance of SC-CCES is better than that of TC-CCES when energy releasing pressure is larger than 21 MPa.

Fig. 7 shows that transcritical CO_2 is better under a releasing pressure of ~20-22 MPa, but SC-CCES becomes better under a high pressure. The reason is that the CO_2 enthalpy will decrease with the increase in pressure at the same temperature. Moreover, the enthalpy difference between different pressures also gradually decreases along with the increase in pressure (cf. Fig. 8).

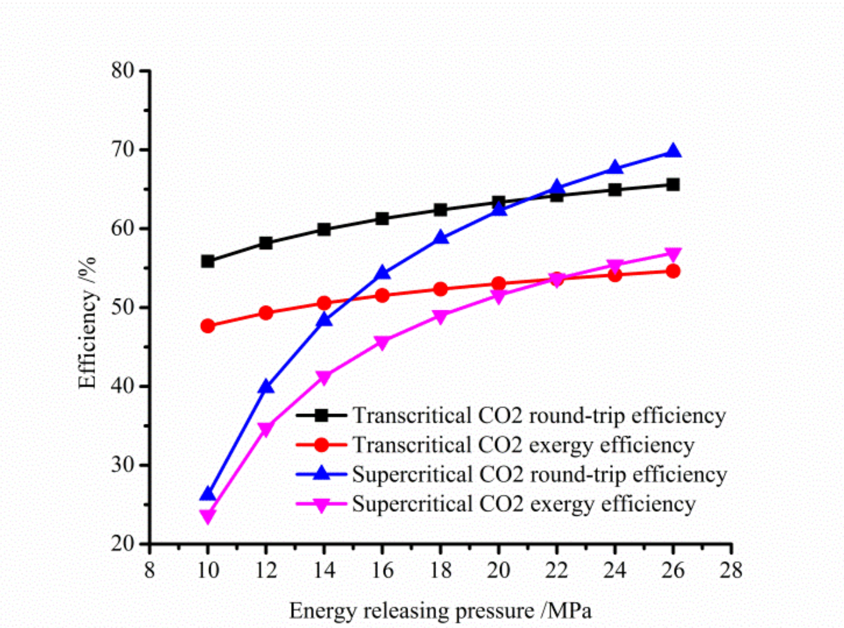

Fig. 7. Effect of energy releasing pressure on round-trip efficiency and exergy efficiency.

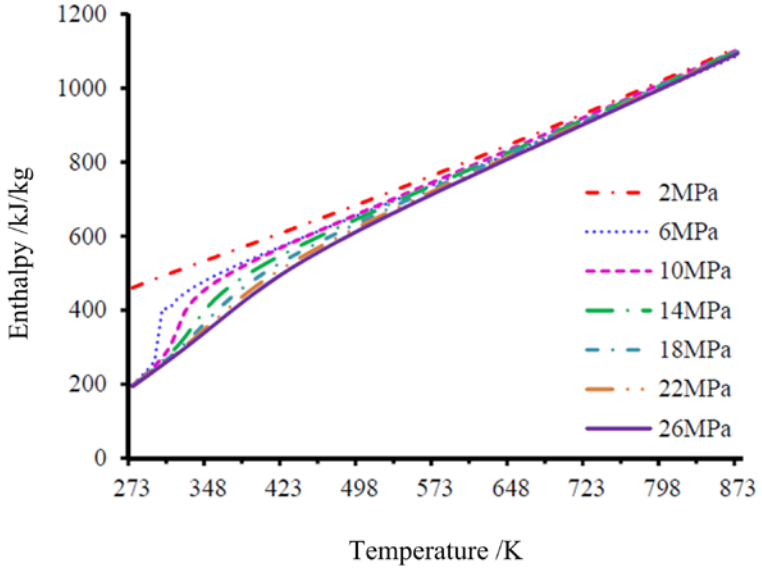

Fig. 8. The *h*-*T* curves for CO_2.

In Fig. 7, the outlet pressure of turbine is constant, so that the input work is constant in the compression process, the input thermal energy and output work will change with the variations of releasing pressure. For supercritical $CO_{2,}$ less thermal energy is needed and more output work is produced with the increase in releasing pressure, and the increasing rate of output work is also higher than that of transcritical CO_2. When the releasing pressure is lower, the supercritical CO_2 need more heat energy and produce less output work compared with transcritical CO_2. Therefore, transcritical CO_2 is better when the releasing pressure is low, but supercritical CO_2 becomes better at high pressure.

Fig. 9 shows the effect of energy releasing pressure on energy storage density. As shown in the preceding analysis, energy storage density is determined by the work output of the turbine train, as well as the outlet pressure of the turbine train and the compressor train. The increase in energy release pressure will increase the work output of the turbine train, and the pressure difference in the high-pressure reservoir will be reduced which results in smaller volume requirement for the high-pressure reservoir; hence the energy storage densities of TC-CCES and SC-CCES both increase with increase in energy release pressure.

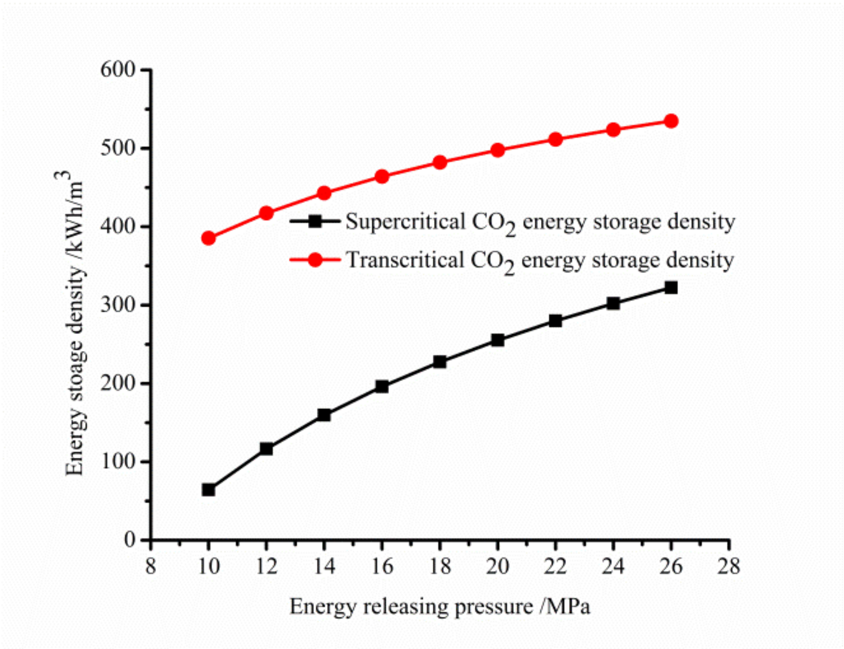

Fig. 9. Effect of energy releasing pressure on energy storage density.

The effect of energy releasing pressure on the exergy destruction rate of the main components is shown in Fig. 10. For TC-CCES and SC-CCES, a greater portion of exergy destruction occurred in He and RE, and they also have the similar trend with the variations in energy releasing pressure. The exergy destruction rate of RE in TC-CCES and SC-CCES decreases with the increase in the energy releasing pressure, whereas that of HE exhibits the opposite trend.

From Fig. 10, we can find that the significant differences between TC-CCES and SC-CCES are that (1) the transcritical exergy destruction rate is larger than that of supercritical CO_2 except in the HS component, and (2) the highest exergy destruction rate happens in different components.

The lower exergy destruction rate of supercritical CO_2 is caused by the fact that for supercritical CO_2, both the input energy and output work are lower than that of transcritical CO_2, so that the exergy destruction rate of supercritical CO_2 is lower.

The reason that the highest exergy destruction rate happened in different components in transcritical versus supercritical CO_2 is that the injection temperature of the high-pressure reservoir is much different between the transcritical CO_2 and supercritical CO_2. As shown in Fig. 2, and in Tables 3 and 4, we can find that the injection pressure of the high-pressure reservoir is equal for the transcritical CO_2 and supercritical CO_2, but the injection temperature of supercritical CO_2 is higher than that of transcritical CO_2. So there is a higher exergy destruction rate in the HS in the compressed supercritical CO_2 energy storage system.

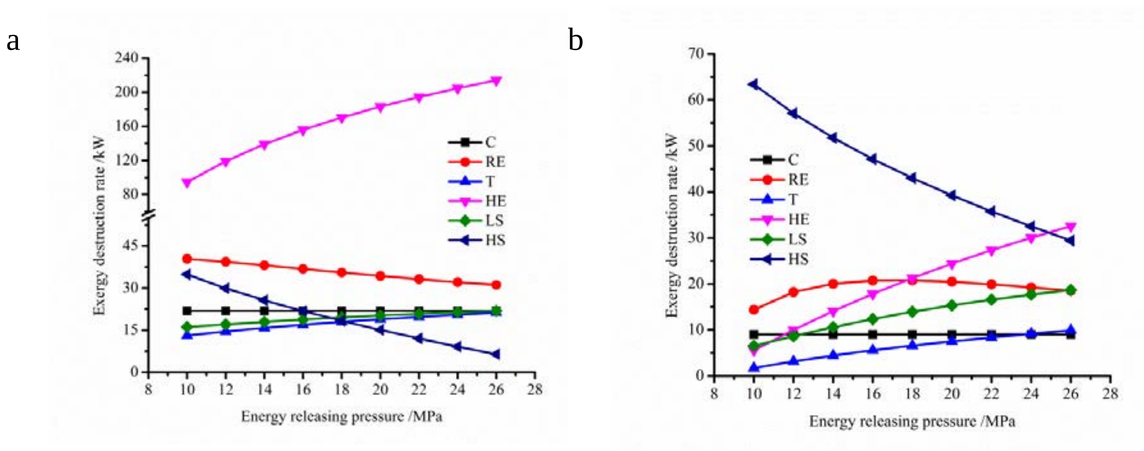

Fig. 10. Effect of energy release pressure on exergy destruction rate. a. Transcritical compressed CO_2 energy storage. b. Supercritical compressed CO_2 energy storage. C = compressor; RE = recuperator; T = turbine; HE = heater; LS = low pressure reservoir; and HS = high pressure reservoir.

5.2.3. Effects of pressure of low pressure reservoir

Fig. 11 shows the effect of the pressure of the low-pressure reservoir on the round-trip efficiency and exergy efficiency of TC-CCES and SC-CCES. It indicates that the pressure of the low-pressure reservoir exerts a larger influence on round-trip efficiency and exergy efficiency for TC-CCES and SC-CCES. The round-trip efficiency and exergy efficiency will firstly decrease, and then increase with increase in pressure of the low-pressure reservoir. This phenomenon is caused by the properties of CO_2. As shown in Fig. 12, both input work of the compressor and output work of the turbine decrease along with increase in pressure of the low-pressure reservoir, but the reduction of output work is greater than the decrease of input work of the compressor. Thus the system performance decreases when the storage system runs at transcritical state. Moreover, when the system runs at supercritical state, the compressibility factor of supercritical CO_2 ranges from 0.2-0.5, which means that less compression work can be consumed in the compression process[43]. Therefore, the reduction of input work will dramatically decrease compared with that at transcritical state. Fig. 13 shows the variations in energy storage density with the increase in pressure of low pressure reservoir. It illustrates that the energy storage density decreases with the increase in pressure of low pressure reservoir. Fig. 14 shows the effect of pressure of low pressure reservoir on exergy destruction rate, which indicates that the exergy destruction rates of HE decrease along with the increase in pressure of the low-pressure reservoir. And when the pressure of the low pressure reservoir is higher than 8 MPa, there is a larger decrease in exergy destruction rate of each component except HS.

The phenomenon we have observed is that performance of SC-CCES can be explained by the properties of supercritical CO_2 and configurations of the energy storage system. Because of the larger mass density and configurations of SC-CCES relative to transcritical CO_2, the input work in compression and the temperature difference in the heater can be reduced. Moreover, the output work in expansion will be increased due to the higher inlet temperature and pressure of the turbine and the higher exhaust temperature caused by a lower pressure ratio will reduce the amount of heat in the heater. Therefore the round-trip efficiency, exergy efficiency, and energy storage density will increase, whereas the exergy destruction rate of heater decreases.

For Figs. 11-14, the pressure range 6.5-8 MPa shows a different mechanism, which is caused by the thermodynamic properties of CO_2. For CO_2, the critical point is 7.39 MPa and 304.25 K. the thermodynamic properties of CO_2 and supercritical CO_2 are very different. Especially around the critical point, the thermodynamic properties of CO_2 will greatly change with changes in P and T[43]. Therefore, the compression work can be substantially decreased, as shown in Fig.12.

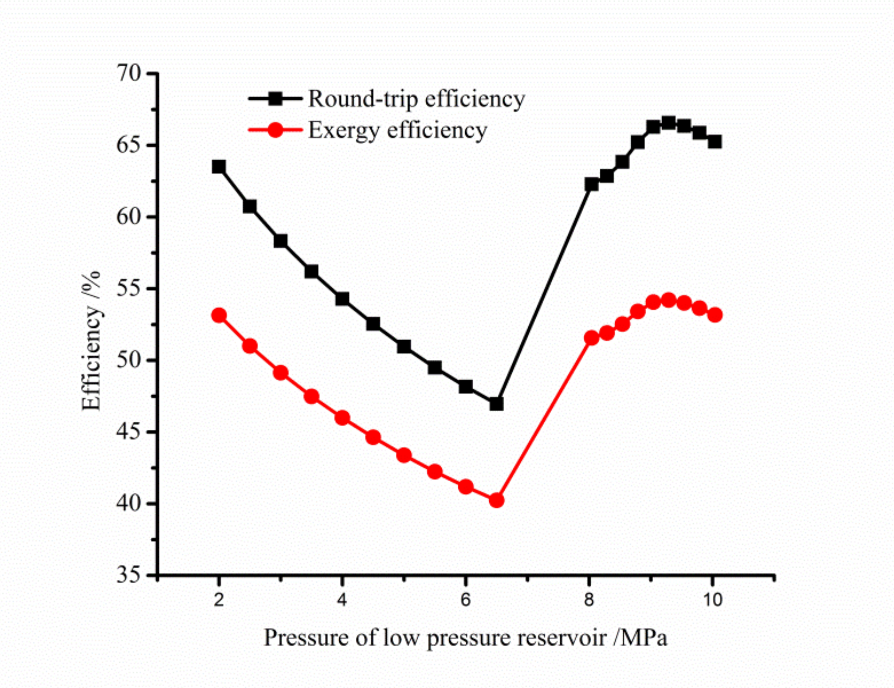

Fig. 11. Effect of pressure of low pressure reservoir on round-trip efficiency and exergy efficiency.

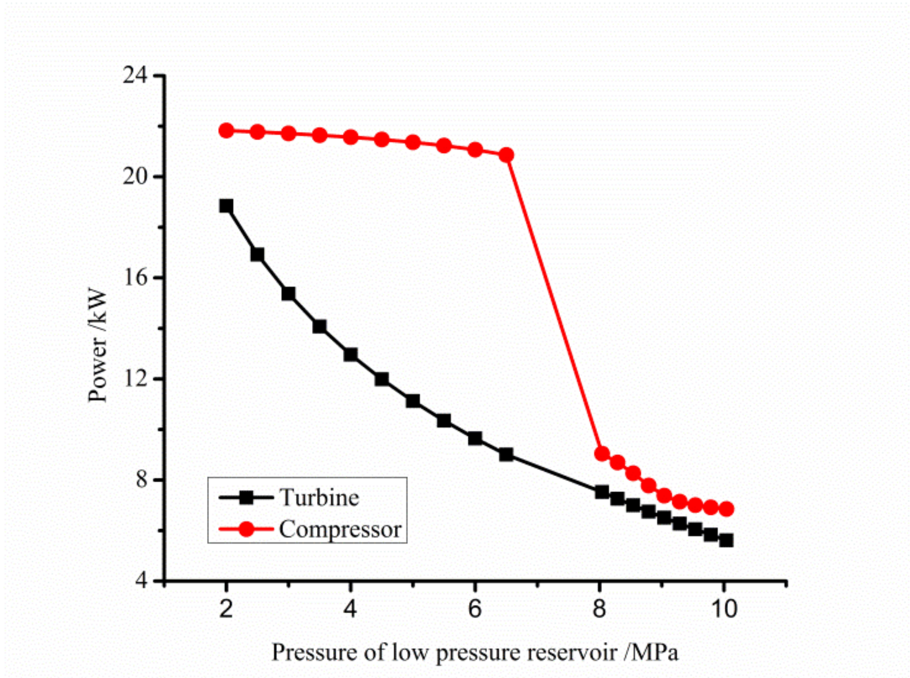

Fig. 12. Effect of pressure of low pressure reservoir on power input and output.

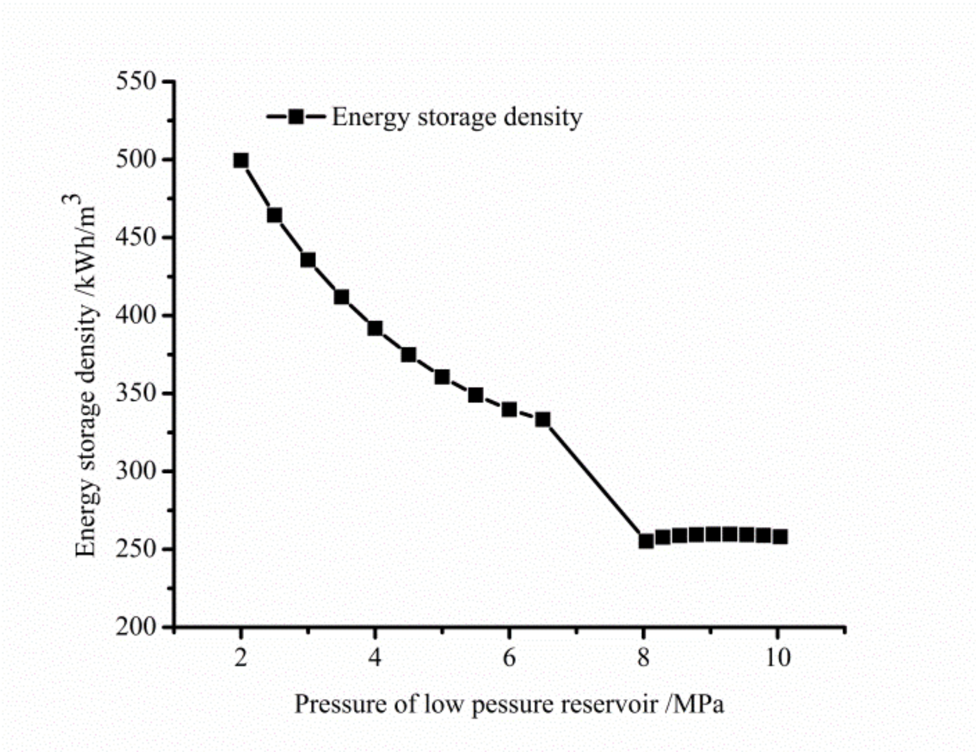

Fig. 13. Effect of pressure of low pressure reservoir on energy storage density.

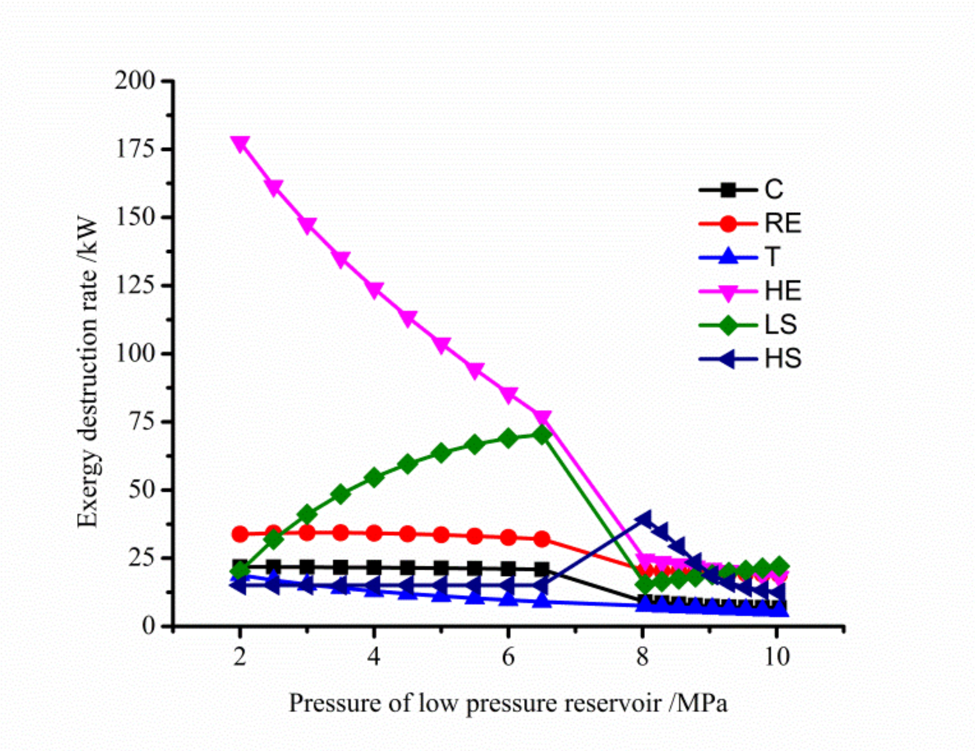

Fig. 14. Effect of pressure of low pressure reservoir on exergy destruction rate. C = compressor; RE = recuperator; T = turbine; HE = heater; LS = low pressure reservoir; and HS = high pressure reservoir.

6. Conclusions

A thermodynamic analysis is carried out of a system consisting of transcritical and supercritical compressed CO_2 energy storage using two saline aquifers as reservoirs, including energy analysis, exergy analysis, and parametric analysis. The main conclusions are summarized as follows:

(1) According to the energy and exergy analysis, the proposed compressed CO_2 energy storage system with two saline aquifers as reservoirs has a larger energy storage density (497.68 kWh/m^3 for transcritical CO_2 and 255.20 kWh/m^3 for supercritical CO_2 compared to CAES (2-20kWh/m^3) and an acceptable round-trip

efficiency (63.35% for transcritical CO_2 and 62.28% for supercritical CO_2) and exergy efficiency (53.02% for transcritical CO_2, and 51.56% for supercritical CO_2) compared with conventional CAES (81.7%[38]).

(2) The use of compressed transcritical CO_2 for energy storage results in a higher round-trip efficiency, exergy efficiency and energy storage density, but the configuration of SC-CCES is simpler compared with TC-CCES.

(3) The energy release pressure has a positive effect on the three indicators including round-trip efficiency, exergy efficiency, and energy storage density forTC-CCES and SC-CCES. The performance of the two energy storage systems will become better with the increase in energy release pressure.

(4) The pressure of the low-pressure reservoir has a large effect on round-trip efficiency and exergy efficiency, especially when the pressure is below 8 MPa. Specifically, for TC-CCES, the round-trip efficiency and exergy efficiency dramatically decrease, whereas the energy storage density will decrease along with the increase in pressure of low pressure reservoir.

We note that for the TC-CCES, the low-pressure reservoir needs to be much shallower and larger than the supercritical CO_2 energy storage reservoir. Therefore it may pose larger potential environmental impacts, (for instance to potable groundwater), than the second system. Also, the hazard of induced seismicity and triggered seismicity may exist in both cyclic injection processes. These issues and others such as, how to reduce brine production to a minimum,, or the hydro-geo-mechanical limitations of the saline aquifer reservoirs, and the optimal cycling time given that transient pressure gradients will exist around the injection and production wells[11] are key questions outside the scope of this study that should be addressed in the future.

Acknowledgements

The paper is supported by the National Nature Science Fund of China (No.51276059), Fundamental Research Funds for the Central Universities of China (No. 2014XS27) and China Scholarship Council (No.1510200035). Additional support came from Lawrence Berkeley National Laboratory supported by the U.S. Department of Energy under Contract No. DE-AC02-05CH11231.

References

[1] Lund H, Salgi G. The role of compressed air energy storage (CAES) in future sustainable energy systems. Energy Convers Manage 2009; 50(5): 1172-1179.

[2] Liu J L, Wang J H. A comparative research of two adiabatic compressed air energy storage systems. Energy Convers Manage 2016;108: 566-578.

[3] Carrasco J M, Franquelo L G, Bialasiewicz J T, Galvan E, Portillo Guisado R C, Prats M A M, et al. Power-electronic systems for the grid integration of renewable energy sources: A survey. IEEE Trans Ind Electron 2006; 53: 1002-1016.

[4] Díaz-González F, Sumper A, Gomis-Bellmunt O, Villafafila-Robles R. A review of energy storage technologies for wind power applications. Renew Sustain Energy Rev 2012; 16(4): 2154-2171.

[5] Mahlia T M I, Saktisahdan T J, Jannifar A, Hasan M H, Matseelar H S C. A review of available methods and development on energy storage; technology update. Renew Sustain Energy Rev 2014; 33: 532-545.

[6] De Bosio F, Verda V. Thermoeconomic analysis of a Compressed Air Energy Storage (CAES) system integrated with a wind power plant in the framework of the IPEX Market. Appl Energy 2015; 152: 173-182.

[7] Cleary B, Duffy A, O'connor A, Conlon M, Fthenakis V. Assessing the economic benefits of compressed air energy storage for mitigating wind curtailment. IEEE Trans Sustain Energy 2015; 6(3): 1021-1028.

[8] Arabkoohsar A, Machado L, Koury R N N. Operation analysis of a photovoltaic plant integrated with a compressed air energy storage system and a city gate station. Energy 2016; 98: 78-91.

[9] Arabkoohsar A, Machado L, Farzaneh-Gord M, Koury R N N. The first and second law analysis of a grid connected photovoltaic plant equipped with a compressed air energy storage unit. Energy 2015; 87: 520-539.

[10] Long-term energy storage with compressed air storages.
<http://ees-magazine.com/long-term-energy-storage-with-compressed-air-storages/>

[11] Oldenburg C M, Pan L. Porous Media Compressed-Air Energy Storage (PM-CAES): Theory and Simulation of the Coupled Wellbore–Reservoir System. Transport Porous Med 2013; 97(2): 201-221.

[12] Buffa F, Kemble S, Manfrida G, Milazzo A. Exergy and exergoeconomic model of a ground-based CAES plant for peak-load energy production[J]. Energies 2013; 6(2): 1050-1067.

[13] Proczka J J, Muralidharan K, Villela D, Simmons J H, Frantziskonis G. Guidelines for the pressure and efficient sizing of pressure vessels for compressed air energy storage. Energy Convers Manage 2013; 65: 597-605.

[14] Zhang Y, Yang K, Li X, Xu J. The thermodynamic effect of thermal energy storage on compressed air energy storage system. Renew Energy 2013; 50: 227-235.

[15] Zhang Y, Yang K, Li X, Xu J. The thermodynamic effect of air storage chamber model on Advanced Adiabatic Compressed Air Energy Storage System. Renew Energy 2013; 57: 469-478.

[16] Jubeh N M, Najjar Y S H. Green solution for power generation by adoption of adiabatic CAES system. Energy Convers Manage 2012; 44: 85-89.

[17] Najjar Y S H, Zaamout M S. Performance analysis of compressed air energy storage (CAES) plant for dry regions. Energy Convers Manage 1998; 39(15): 1503-1511.

[18] Crotogino F, Mohmeyer K U, Scharf R. Huntorf CAES: More than 20 years of successful operation, Orlando, Florida, USA; 2001.

[19] Safaei H, Keith D W. Compressed air energy storage with waste heat export: An Alberta case study. Energy Convers Manage 2014; 78: 114-124.

[20] Luo X, Wang J, Krupke C, Wang Y, Sheng Y, Li J, et al. Modelling study, efficiency analysis and optimisation of large-scale Adiabatic Compressed Air Energy Storage systems with low-temperature thermal storage. Appl Energy 2016; 162: 589-600.

[21] Guo Z, Deng G, Fan Y, Chen G. Performance optimization of adiabatic compressed air energy storage with ejector technology. Appl Therm Eng 2016; 94: 193-197.

[22] Li Y, Wang X, Li D, Ding Y. A trigeneration system based on compressed air and thermal energy storage. Appl Energy 2012; 99: 316-323.

[23] Nielsen L, Leithner R. Dynamic Simulation of an Innovative Compressed Air Energy Storage Plant-Detailed Modelling of the Storage Cavern[J]. WSEAS Trans Power Sys 2009; 4(8): 253-263.

[24] Yao E, Wang H, Wang L, Xi G, Marechal F. Thermo-economic optimization of a combined cooling, heating and power system based on small-scale compressed air energy storage. Energy Convers Manage 2016; 118: 377-386.

[25] Tessier M J, Floros M C, Bouzidi L, Narine S S. Exergy analysis of an adiabatic compressed air energy storage system using a cascade of phase change materials. Energy 2016; 106: 528-534.

[26] Simpson M C, Garvey S D, Pimm A, Kantharaj B, Cardenas B, Garvey J E. Integrating solar thermal capture with compressed air energy storage, London, UK; 2016.

[27] Li Y, Sciacovelli A, Peng X, Radcliffe J, Ding Y. Integrating compressed air energy storage with a diesel engine for electricity generation in isolated areas. Appl Energy 2016; 171: 26-36.

[28]Zhang Y, Yang K, Hong H, Zhong X, Xu J. Thermodynamic analysis of a novel energy storage system with carbon dioxide as working fluid. Renew Energy 2016; 99: 682-697.

[29] Chen H, Cong T N, Yang W, Tan C, Li Y, Ding Y. Progress in electrical energy storage system: A critical review. Prog Nat Sci 2009; 19(3): 291-312.

[30] Kim Y M, Shin D G, Favrat D. Operating characteristics of constant-pressure compressed air energy storage (CAES) system combined with pumped hydro storage based on energy and exergy analysis. Energy 2011; 36(10): 6220-6233.

[31] Guo H, Xu Y, Chen H, Zhou X. Thermodynamic characteristics of a novel supercritical compressed air energy storage system. Energy Convers Manage 2016; 115: 167-177.

[32] Pimm A J, Garvey S D, de Jong M. Design and testing of energy bags for underwater compressed air energy storage. Energy 2014; 66: 496-508.

[33] Jannelli E, Minutillo M, Lavadera A L, Falcucci G. A small-scale CAES (compressed air energy storage) system for stand-alone renewable energy power plant for a radio base station: A sizing-design methodology. Energy 2014; 78: 313-322.

[34] Dostal V. A supercritical carbon dioxide cycle for next generation nuclear reactors. PhD dissertation, Massachusetts Institute of Technology. These N MIT-ANP-TR-100; 2004.

[35] Wang M, Zhao P, Wu Y, Dai Y. Performance analysis of a novel energy storage system based on liquid carbon dioxide. Appl Therm Eng 2015; 91: 812-823.

[36] Zhou Q, Birkholzer J T, Tsang C F, Rutqvist J. A method for quick assessment of CO_2 storage capacity in closed and semi-closed saline formations. Int J Greenh Gas Con 2008; 2(4): 626-639.

[37] Cayer E, Galanis N, Desilets M, Nesreddine H, Roy P. Analysis of a carbon dioxide transcritical power cycle using a low temperature source. Appl Energy 2009; 86(7): 1055-1063.

[38] Succar, Samir, and Robert H. Williams. Compressed air energy storage: theory, resources, and applications for wind power. Report no. 8, Princeton environmental institute; 2008.

[39] Kim Y M, Lee J H, Kim S J, Favrat D. Potential and evolution of compressed air energy storage: energy and exergy analyses. Entropy 2012; 14(8): 1501-1521.

[40] Liu H, He Q, Saeed S B. Thermodynamic analysis of a compressed air energy storage system through advanced exergetic analysis. J Renew Sustain Energy 2016; 8(3): 034101.

[41] Wang L, Yang Y, Morosuk T, Tsatsaronis G. Advanced thermodynamic analysis and evaluation of a supercritical power plant. Energies 2012; 5(6): 1850-1863.

[42] Welcome to CoolProp. <http://www.coolprop.org/>

[43] Ahn Y, Bae S J, Kim M, Cho S K, Baik S, Lee J I, et al. Review of supercritical CO_2 power cycle technology and current status of research and development. Nuc Eng Technol 2015; 47(6): 647-661.